# High-Mobility Ambipolar Transport in Organic Light-Emitting Transistors

Dinelli, Franco; Capelli, Raffaella; Loi, Maria A.; Murgia, Mauro; Muccini, Michele; Facchetti, Antonio; Marks, Tobin J.

*Published in:*
Advanced materials

*DOI:*
10.1002/adma.200502164

ADVANCED MATERIALS

DOI: 10.1002/adma.200502164

# High-Mobility Ambipolar Transport in Organic Light-Emitting Transistors**

By *Franco Dinelli*,* *Raffaella Capelli*, *Maria A. Loi*, *Mauro Murgia*, *Michele Muccini*, *Antonio Facchetti*, and *Tobin J. Marks*

Today organic materials are routinely employed for the fabrication of light-emitting devices (OLEDs) and thin-film transistors (OTFTs), with the first technological realizations already having reached the market.[1] Moreover, OTFTs with unipolar mobility values comparable to those of amorphous silicon (1 $cm^2 V^{-1} s^{-1}$) have now been demonstrated.[2] Applications impacting display technologies and those sectors where low cost is a key factor and low performance is acceptable include electronic paper and radio-frequency identification (RF-ID) products. In a recent development, OTFTs also exhibiting electroluminescence (EL) have been successfully demonstrated.[3,4] Organic light-emitting transistors (OLETs) represent a significant technological advance by combining two functionalities, electrical switching and light emission, in a single device, thus significantly increasing the potential applications of organic semiconductors. In particular, if appropriate materials can be introduced, OLETs offer an ideal structure for improving the lifetime and efficiency of organic light-emitting heterostructures due to the intrinsically different driving conditions and charge-carrier balance compared to conventional OLEDs. Potential applications of OLETs include flat-panel display technologies, lighting, and, ultimately, easily fabricated organic lasers.

The first OLET prototypes were unipolar transport devices, and recombination was expected to take place in close proximity to the metallic drain electrode where efficiency-depleting exciton quenching is also likely to occur. To avoid this significant device deficiency and to instead generate EL nearer the center of the channel, OLETs with ambipolar charge transport would be highly desirable. Furthermore, balanced ambipolar conduction is crucial for maximizing exciton recombination through efficient electron–hole balancing. Up to now various solutions have been proposed: single ambipolar materials[5–8] and two-component coevaporated[9] or layered[10,11] structures. In coevaporated films, two materials are simultaneously sublimed to form bulk heterojunctions. However, carrier transport is unbalanced and the mobility values are below $10^{-3}$ $cm^2 V^{-1} s^{-1}$.[9b] Devices employing a polymer film showing intrinsic ambipolar transport have also been reported but with mobility values for both charge carriers around $10^{-4}$ $cm^2 V^{-1} s^{-1}$.[8]

In this paper we report OLETs based on two-component layered structures that have balanced ambipolar transport and mobility values as large as $3 \times 10^{-2}$ $cm^2 V^{-1} s^{-1}$. These devices are realized by sequentially depositing p-type (α,ω-dihexyl-quaterthiophene, DH4T) and n-type films (*N*,*N*′-ditridecylperylene-3,4,9,10-tetracarboxylic diimide, PTCDI-$C_{13}H_{27}$, P13). The combination with the highest mobility and most-balanced transport is obtained with DH4T grown in direct contact with the dielectric. For comparison, we have also employed pentacene in place of DH4T as the p-type material and showed that unbalanced ambipolarity is obtained. Morphological analysis of the outermost and buried layers, performed by laser scanning confocal microscopy (LSCM), allows selective imaging of materials with energetically separated photoluminescence (PL) spectra. Importantly, it is shown that 'growth compatibility' between the n- and p-type materials is essential in forming a continuous interface and thereby controlling the resulting OLET optoelectronic-response properties.

Each OLET material was first evaluated in a single layer in a top source–drain contact OTFT. As substrates we employed heavily doped silicon wafers with thermally grown oxides. Surface treatments such as octadecyltrichlorosilane or hexamethyldisilazane did not result in substantial improvement in the device performance. Parameters such as substrate temperature ($T_{sub}$) and evaporation rate were varied to optimize electrical characteristics. The optimum growth conditions were found to be: $T_{sub} = 90\,°C$ and rate = 0.1 $Å\,s^{-1}$ for DH4T, and $T_{sub} = 25\,°C$ and rate = 0.1 $Å\,s^{-1}$ for P13. In Table 1, the mobility ($\mu$) and threshold-voltage ($V_{th}$) values obtained are summarized. These are comparable to the highest values reported in the literature.[12,13] The DH4T devices were stable even

[*] Dr. F. Dinelli, Dr. R. Capelli, Dr. M. A. Loi, Dr. M. Murgia, Dr. M. Muccini
Consiglio Nazionale delle Ricerche (CNR)
Istituto per lo Studio dei Materiali Nanostrutturati (ISMN)
via P. Gobetti 101, 40129 Bologna (Italy)
E-mail: franco.dinelli@ipcf.cnr.it
Dr. A. Facchetti, Prof. T. J. Marks
Department of Chemistry and the Materials Research Center
Northwestern University
2145 Sheridan Road, Evanston, IL 60208 (USA)

[**] The authors thank R. Zamboni for stimulating discussions and P. Fancello for technical support. This work was supported at Bologna by the EU under the project FP6-IST-015034 (OLAS) and by the Italian Ministry MIUR under the project FIRB-RBNE033KMA ("Composti molecolari e materiali ibridi nanostrutturati con proprietà ottiche risonanti e non risonanti per dispositivi fotonici"), and at Northwestern by the NASA Institute for Nanoelectronics and Computing (NCC2-3163) and NSF through the Northwestern MRSEC (DMR-0076097).

**Table 1.** $\mu$ and $V_{th}$ values of single-layer and bilayer devices.

| Sample | $\mu^n$ [$cm^2 V^{-1} s^{-1}$] | $V_{th}^n$ [V] | $\mu^p$ [$cm^2 V^{-1} s^{-1}$] | $V_{th}^p$ [V] |
|---|---|---|---|---|
| DH4T | – | – | 0.04 | –2 |
| P13 | 0.15 | 20 | – | – |
| P13 [a] | 0.03 | 30 | – | – |
| DH4T–P13 | 0.03 | 2 | 0.03 | –8 |
| P13–DH4T | 0.04 | 9 | 0.002 | –10 |

[a] Data obtained from a device after annealing at 90 °C for 60 min.

when characterized in air, exhibiting low hysteresis and small $V_{th}^p$ (threshold voltage for p-type behavior) shifts. $V_{th}^p$ typically ranged from –1 to –5 V. In contrast, the P13 devices were more sensitive to air exposure, but rapidly recovered their electrical characteristics on being subjected to vacuum. $V_{th}^n$ (threshold voltage for n-type behavior) typically ranged from 10 to 20 V; these are relatively small values, although electron-injection optimization was not pursued. Here we employed Au electrodes for ease of fabrication, although using Ca or Al should result in improved electron injection.[14] The hysteresis and $V_{th}^n$ shifts were always greater than in DH4T devices. EL in single-layer OTFTs was observed for P13 but not for DH4T. Since they are unipolar devices, EL is expected to occur at the source/electrode interface by a mechanism similar to that previously established in tetracene-based OLETs.[3,4]

Layered structures were grown by sequentially depositing p- and n-type films. In a DH4T–P13 device, DH4T was evaporated directly onto the dielectric (see schematic in Fig. 1A), whereas, in the P13–DH4T device, P13 was directly grown on the dielectric. The DH4T–P13 combination exhibited the most-balanced ambipolarity with the highest mobilities ($\mu \sim 3 \times 10^{-2}$ $cm^2 V^{-1} s^{-1}$ for both types of conduction). $\mu^p$ (mobility for p-type behavior) did not vary substantially with respect to the single-layer devices, while $\mu^n$ (mobility for n-type behavior) decreased by one order of magnitude despite the fact that P13 growth was carried out under optimized conditions. This is likely to be due to differences in growth modality on a surface different from silicon oxide in both chemical composition and morphology.

The ambipolar nature of charge transport can be clearly observed in the output characteristics (Fig. 1B). Thus, injection of electrons from the drain is obtained for $V_{ds} < (V_{gs} - V_{th}^n)$, where $V_{ds}$ is the drain–source voltage and $V_{gs}$ is the gate–source voltage. At $V_{gs} = 0$ V, for instance, the drain current ($I_d$) diverges with decreasing $V_{ds}$. For decreasing $V_{gs}$, electron injection from the drain is shifted to lower and lower values of $V_{ds}$, holes are injected from the source, and $I_d$ curves saturate at $V_{ds} = (V_{gs} - V_{th}^p)$, as in unipolar OTFTs. Symmetrically, as shown in Figure 1C, injection of holes from the drain is obtained for $V_{ds} > (V_{gs} - V_{th}^p)$. At $V_{gs} = 0$ V, $I_d$ diverges with increasing $V_{ds}$. For increasing $V_{gs}$, hole injection from the drain is shifted to higher and higher $V_{ds}$, electrons are injected from the source, and $I_d$ curves saturate at $V_{ds} = (V_{gs} - V_{th}^n)$. The

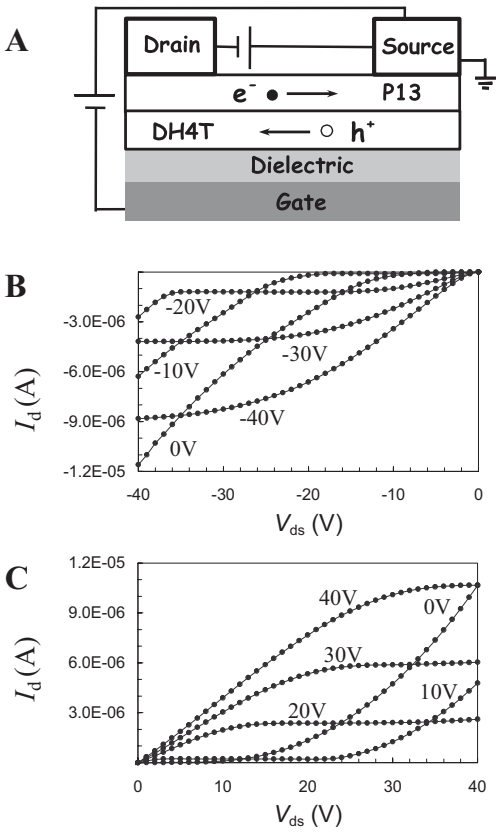


**Figure 1.** A) Schematic of an OLET device based on a DH4T–P13 bilayer. B) Output curves ($I_d$ vs. $V_{ds}$) obtained from a DH4T–P13 device operating in a p-type configuration or C) in an n-type configuration. $V_{gs}$ values are reported beside each curve. $I_d$ = drain current; $V_{ds}$ = drain–source voltage; $V_{gs}$ = gate–source voltage.

good balance achieved is best appreciated from the symmetry in the transfer curves obtained in the saturation regime (Fig. 2A,B). Under these biasing conditions, electrons are injected from the drain for $V_{gs} > (V_{ds} + V_{th}^n)$, whereas holes are injected from the drain for $V_{gs} < (V_{ds} + V_{th}^p)$. This performance is comparable to the highest performance reported in the literature for the case of pentacene and perfluoropentacene ($\mu = 3 \times 10^{-2}$ $cm^2 V^{-1} s^{-1}$ for both types of conduction).[11] However, the latter combination cannot be usefully employed for EL applications. It will be seen in the following discussion that in the present case, state-of-the-art ambipolar conduction is accompanied by substantial EL emission.

The sequence of deposition can be changed by first subliming P13 onto the dielectric and then DH4T onto P13. However, these devices exhibit unbalanced transport; electron transport is more pronounced than hole transport (Fig. 2C,D). The transfer curves are not as symmetrical as in Figure 2A and B. $I_d$ at large $V_{gs}$ (due to electrons) is larger by one order of magnitude with respect to $I_d$ at low $V_{gs}$ (due to holes). In terms of mobility values, $\mu^p$ drops by one order of magnitude and $\mu^n$ is substantially unchanged with respect to that of the DH4T–P13 structures. However, $\mu^n$ is one order of magnitude smaller compared to single-film devices, although the P13

  

ADVANCED MATERIALS

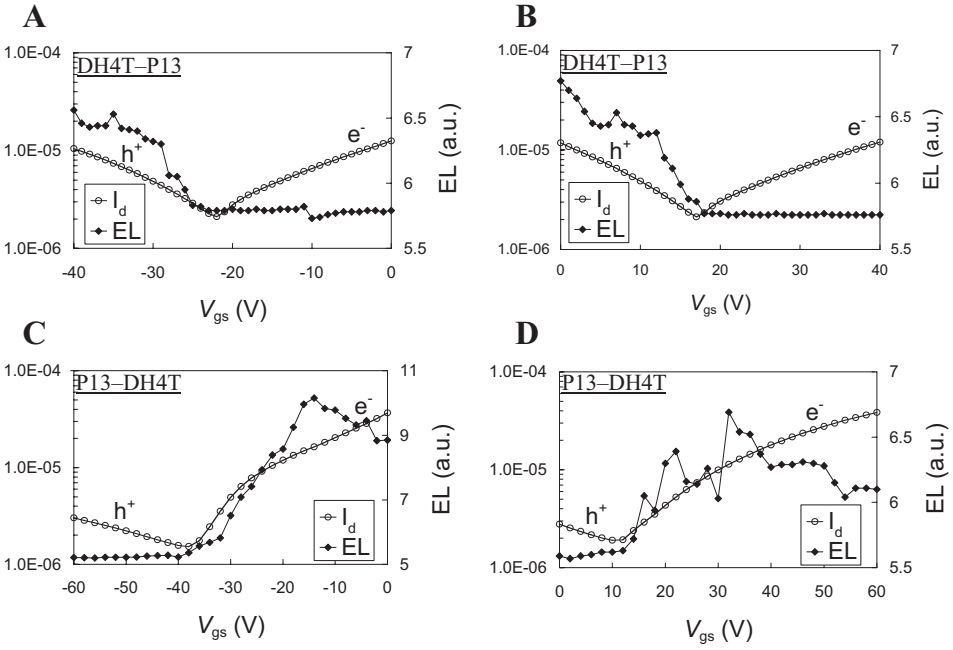


**Figure 2.** Transfer curves ($I_d$ vs. $V_{gs}$ at fixed $V_{ds}$) obtained in the saturation regime. EL data are also plotted. $I_d$ is plotted as absolute values on a logarithmic scale. A,B) Data obtained from a DH4T–P13 device; $V_{ds}$ is equal to ±40 V for positive and negative $V_{gs}$. C,D) Data obtained from a P13–DH4T device; $V_{ds}$ is equal to ±60 V for positive and negative $V_{gs}$.

layer is grown under optimal conditions. The reason for this lies in the fact that, after P13 growth at 25 °C, substrate heating to 90 °C is required for DH4T growth to obtain p-type behavior. This substrate heating reveals itself as detrimental to n-type performance and is equivalent to thermal annealing as shown in Table 1, where we report values obtained for single-layer P13 devices maintained at 90 °C for one hour after growth.

In Figure 2, along with the $I_d$ transfer curves, we plotted EL data. For structures with DH4T placed at the bottom (Fig. 2A,B), EL was observed when holes were flowing through the device, injected either from the drain or the source electrode. In contrast, for P13 placed at the bottom (Fig. 2C,D), EL is observed when electrons are flowing through the device, injected either from the drain or the source electrode. EL also depends on the device history (number of cycles and previous polarization), particularly for P13–DH4T devices where a large asymmetry was also observed. These observations can be generalized by stating that EL occurs only when the layer in direct contact with the dielectric is conductive. From the energetics of the single materials, the EL emission of the bilayer structure is expected to originate from P13. In order to provide a full explanation for this phenomenon further investigations are required.

One important issue here is to establish the extent of Au penetration into the organic layer. Metal penetration into organic films is common, and various solutions to this problem have been proposed, such as increasing the distance between the crucible and the target or cooling the target.[15] For the fabrication of our devices, the target was positioned at a distance of approximately 50 cm. We also cooled the substrate to liquid-nitrogen temperature. However, no noticeable difference in device performance is observed. A second important issue to be clarified was the degree of interpenetration of the two organic layers. Charge-accumulation regions are localized next to the organic/dielectric and organic/organic interfaces.[16] The former is largely governed by the silicon oxide roughness and, possibly, by the surface chemical composition, while the latter is governed by the morphology of the bottom organic layer. Characterization of such interfaces would be crucial to ascertaining the extent of interaction between the two accumulation regions.

In order to explain the variations in the electrical characteristics observed on inverting the deposition sequence in the present experiments, a morphological analysis of the layered structures would be required. However, this can not be achieved by atomic force microscopy or by similar scanning-probe techniques, since they are sensitive only to outer-layer morphology, not to buried interfaces. Therefore, we employed LSCM, in which samples are scanned with a laser and the resulting PL collected. Since P13 and DH4T are characterized by energetically well-separated PL spectra, one or the other material can be selectively imaged. DHT4 PL was collected in the spectral range 515 ± 20 nm, P13 at a wavelength > 600 nm.[9b] Thus, LSCM allows observation of both the outermost and buried layers. From the PL images one can then deduce the morphological characteristics of the various interfaces. Note that, in the case of DH4T–P13 films, DH4T PL can be partially reabsorbed by P13. However, this would only cause attenuation of the signal amplitude when imaging

  

DH4T films. PL from P13 falls in the red region and therefore is not collected.

In Figure 3, it can be seen from the LSCM images that the morphology of the DH4T film grown on P13 is discontinuous compared to that of the DH4T film grown directly on the dielectric. Dark regions are clearly visible; these regions are assigned to holes where DH4T does not cover P13. Note again that both DH4T films were grown at 90 °C. The film texture was even more discontinuous when DH4T was deposited at 25 °C. Variations in PL intensity may be due to either variations in film thickness or variations in grain orientation.[17]

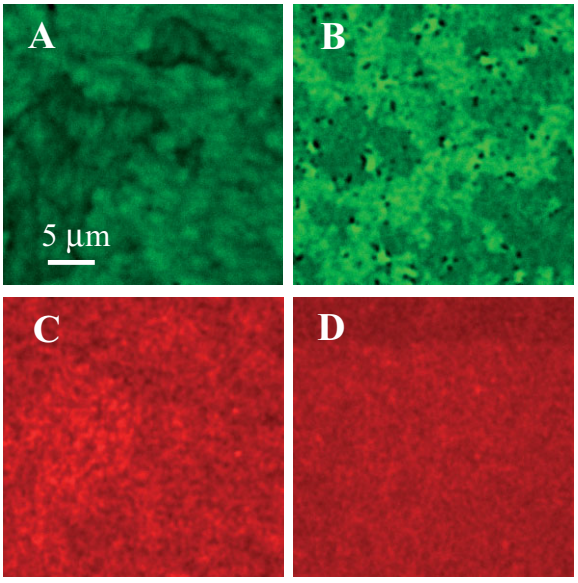


**Figure 3.** 30 μm × 30 μm LSCM images of DH4T–P13 (A,C) and P13–DH4T (B,D) bilayers. The colors represent the PL emission: green in (A,B) from DH4T, red in (C,D) from P13. The detection is centered at 515 ± 20 nm (green channel), and at > 600 nm (red channel).

In marked contrast, the LSCM images in Figure 3 indicate that the P13 films are continuous, independent of whether growth is on the dielectric or on DH4T. Within the resolution limits of LSCM, the morphology is also very similar. Thus, P13 forms continuous films on either silicon oxide or DH4T, but DH4T does not form a continuous film on P13. This result plausibly explains the great differences in device characteristics reported above. Associated with interfacial discontinuity in the organic films is a consequent deterioration in charge-transport efficiency.

To further confirm the importance of the organic/organic interface in the present OLET structure, DH4T was replaced by pentacene as the p-type material. Pentacene is currently the highest-mobility p-type material used in single-layer OTFTs.[2] Pentacene is also known to grow in a layered manner, forming terracelike structures on silicon oxide surfaces.[18] DH4T is instead characterized by a three-dimensional growth pattern with closely adjacent individual crystallites.[19] Pentacene was first investigated in a single-layer configuration. The optimum growth conditions were found to be $T_{sub} = 50$ °C and rate = 0.1 Å $s^{-1}$. Pentacene–P13 devices exhibit unbalanced transport with $\mu^p$ comparable to that of single-layer films (0.2–0.4 $cm^2 V^{-1} s^{-1}$) but with $\mu^n$ dropping by two orders of magnitude (0.002 $cm^2 V^{-1} s^{-1}$). LSCM images of these combinations are displayed in Figure 4. It is evident that, while forming a continuous interface on DH4T, P13 films are discontinuous when deposited on pentacene. The morphology appears to be weblike with empty holes. The continuity deteriorates if the growth parameters are altered, that is, if the substrate temperature is increased above room temperature during P13 deposition. Therefore, choosing two materials to form a smooth and continuous organic/organic interface is challenging, and optimum property combinations are not necessarily obtained by employing materials with substantial mobility values in single-layer configurations alone. For pentacene–P13 devices, EL is also observed. The modality is, however, the same as for devices based on DH4T. Significant EL occurs only when the bottom layer that is in direct contact with the dielectric is conductive.

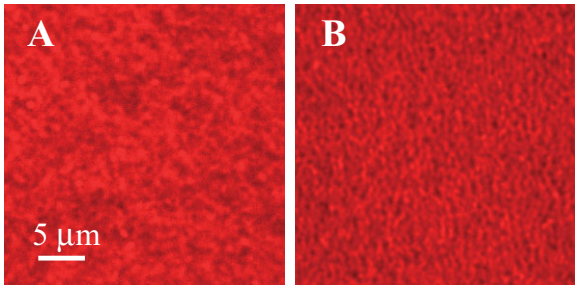


**Figure 4.** 30 μm × 30 μm LSCM images of P13 films grown on top of DH4T (A) and on top of pentacene (B) layers. The detection is centered at > 600 nm (red channel).

In conclusion, OLET devices with balanced ambipolar transport have been obtained by using layered organic structures. The molecules employed are DH4T for the p-type and P13 for the n-type layer. The mobility values are ca. $3 \times 10^{-2}$ $cm^2 V^{-1} s^{-1}$, the highest reported to date for ambipolar OLETs with balanced transport. Morphological analysis by means of confocal PL microscopy indicates that 'growth' compatibility is required in order to form a continuous interface between the two organic films. This compatibility is crucial to controlling the quality of the interface and the resulting optoelectronic properties of the OLETs. Optimum performance is not necessarily achieved by employing materials with the highest mobility values in single-layer devices.

## *Experimental*

Pentacene and P13 were purchased from Aldrich and employed as received. DH4T was synthesized as described in the literature [12b]. The deposition parameters were optimized for each material in a sin-

  

ADVANCED MATERIALS

gle-layer configuration. $T_{sub}$ values for film growth were 90 °C for DH4T, 25 °C for P13, and 50 °C for pentacene. The growth rate was fixed for all materials at 0.1–0.2 Å $s^{-1}$ (0.6–1.2 nm $min^{-1}$). Organic films were deposited at a base pressure of $5 \times 10^{-7}$ mbar (1 bar = 100 000 Pa), each layer having a nominal thickness of 20 nm, as measured with a quartz-crystal microbalance. Differences in the sticking coefficients at these substrate temperatures can be considered to be negligible.

Substrates consisted of heavily doped $n^{++}$ silicon with a layer of thermally grown oxide. The oxide thickness varied from 100 to 300 nm ($C_{ox}$ = 36 and $12 \times 10^{-9}$ F $cm^{-1}$, respectively). No surface treatment was carried out on the oxide apart from cleaning procedures such as sonication in chloroform, acetone, and ultrahigh-purity water in order to remove possible organic contamination.

OLET devices were fabricated in the top-electrode configuration. The electrodes were made of Au deposited at a base pressure of $2 \times 10^{-4}$ mbar at a growth rate of 0.5 Å $s^{-1}$ with the sample held at room temperature or –120 °C. Device geometry factors were the following: width = 10 mm and length = 150 to 600 μm.

Electrical measurements were carried out within an integrating sphere at a base pressure of $1 \times 10^{-4}$ mbar using a photomultiplier for EL measurements. Mobility and threshold-voltage values were evaluated in the saturation regime through the acquisition of Locus Curves. When not limited by the contact resistance at the organic/electrode interfaces, they were also calculated in the linear regime from the transfer curves. The results were essentially indistinguishable.

LSCM was performed with a set-up based on a Nikon Eclipse 2000-E laser-scanning confocal microscope working in the backscattering configuration [20]. PL was excited with a 488 nm $Ar^+$ laser line. Sample imaging was achieved by rastering the laser spot on the sample surface and by detecting, point-by-point, the sample PL with two photomultipliers centered in the green and red spectral range, respectively.

Received: October 10, 2005
Final version: February 14, 2006
Published online: April 24, 2006

[1] a) L. S. Hung, C. H. Chen, *Mater. Sci. Eng., R* **2002**, *39*, 143. b) G. Malliaras, R. Friend, *Phys. Today* **2005**, *58*, 53.

[2] a) S. F. Nelson, Y.-Y. Lin, D. J. Gundlach, T. N. Jackson, *Appl. Phys. Lett.* **1998**, *72*, 1854. b) H. Klauk, M. Halik, U. Zschieschang, G. Schmid, W. Radlik, *J. Appl. Phys.* **2002**, *92*, 5259. c) C. Reese, M. Roberts, M.-M. Ling, Z. Bao, *Mater. Today* **2004**, *7*, 20. d) H. E. Katz, *Chem. Mater.* **2004**, *16*, 4748. e) Y. Sun,Y. Liu, D. Zhu, *J. Mater. Chem.* **2005**, *15*, 53.

[3] A. Hepp, H. Heil, W. Weise, M. Ahles, R. Schmechel, H. von Seggern, *Phys. Rev. Lett.* **2003**, *91*, 157 406.

[4] C. Santato, R. Capelli, M. A. Loi, V. A. L. Roy, P. Stallinga, F. Cicoira, M. Murgia, R. Zamboni, M. Muccini, C. Rost, S. Karg, *Synth. Met.* **2004**, *146*, 329.

[5] T. Yasuda, T. Tsutsui, *Chem. Phys. Lett.* **2005**, *402*, 395.

[6] M.-H. Yoon, S. A. Di Benedetto, A. Facchetti, T. Marks, *J. Am. Chem. Soc.* **2005**, *127*, 1348.

[7] a) T. G. Anthopulos, C. Tanase, S. Setayesh, E. J. Meijer, J. C. Hummelen, P. W. Blom, D. de Leeuw, *Adv. Mater.* **2004**, *16*, 2174. b) E. J. Meijer, D. M. de Leeuw, S. Setayesh, E. van Veneendaal, B.-H. Huisman, P. W. M. Blom, J. C. Hummelen, U. Scherf, T. M. Klapwijk, *Nat. Mater.* **2003**, *2*, 678.

[8] a) J. Zaumseil, R. H. Friend, H. Sirringhaus, *Nat. Mater.* **2006**, *5*, 569. b) J. S. Swensen, C. Soci, A. J. Heeger, *Appl. Phys. Lett.*, **2005**, *87*, 253 511.

[9] a) C. Rost, S. Karg, W. Riess, M. A. Loi, M. Murgia, M. Muccini, *Appl. Phys. Lett.* **2004**, *85*, 1613. b) M. A. Loi, C. Rost-Bietsch, M. Murgia, S. F. Karg, W. Riess, M. Muccini, *Adv. Funct. Mater.* **2006**, *1*, 41.

[10] C. Rost, D. J. Gundlach, S. Karg, W. Riess, *J. Appl. Phys.* **2004**, *95*, 5782.

[11] Y. Sakamoto, T. Suzuki, M. Kobayashi, Y. Gao, Y. Fukai, Y. Inoue, F. Sato, S. Tokito, *J. Am. Chem. Soc.* **2004**, *126*, 8138.

[12] a) P. R. L. Malenfant, C. D. Dimitrakopoulos, J. D. Gelorme, L. L. Kosbar, T. O. Graham, A. Curioni, W. Andreoni, *Appl. Phys. Lett.* **2002**, *80*, 2517. b) A. Facchetti, M. Mushrush, H. E. Katz, T. J. Marks, *Adv. Mater.* **2003**, *15*, 33.

[13] a) K. N. N. Unni, A. K. Pandey, J. M. Nunzi, *Chem. Phys. Lett.* **2005**, *407*, 95. b) D. J. Gundlach, K. P. Pernstich, G. Wilckens, M. Gruter, S. Haas, B. Batlogg, *J. Appl. Phys.* **2005**, *98*, 4502.

[14] L. L. Chua, J. Zaumseil, J.-F. Chang, E. C.-W. Ou, P. K.-H. Ho, H. Sirringhaus, R. H. Friend, *Nature* **2005**, *434*, 194.

[15] A. C. Durr, F. Schreiber, M. Kelsch, H. D. Carstanjen, H. Dosch, *Adv. Mater.* **2002**, *14*, 961.

[16] a) F. Dinelli, M. Murgia, P. Levy, M. Cavallini, F. Biscarini, D. de Leeuw, *Phys. Rev. Lett.* **2004**, *92*, 6802. b) J. Veres, S. Ogier, G. Lloyd, D. de Leeuw, *Chem. Mater.* **2004**, *16*, 4543. c) A. Facchetti, M.-Y. Yoon, T. J. Marks, *Adv. Mater.* **2005**, *17*, 1705.

[17] F. Cicoira, C. Santato, F. Dinelli, M. Murgia, M. A. Loi, F. Biscarini, R. Zamboni, P. Hereman, M. Muccini, *Adv. Funct. Mater.* **2005**, *15*, 375.

[18] J. F. Meyer zu Heringdorf, M. C. Reuter, R. M. Tromp, *Nature* **2003**, *412*, 517.

[19] M. Campione, A. Borghesi, M. Moret, A. Sassella, *J. Mater. Chem.* **2003**, *13*, 1669.

[20] M. A. Loi, E. Da Como, R. Zamboni, M. Muccini, *Synth. Met.* **2003**, *139*, 687.

  